

Performance evaluation of an adsorption refrigeration system powered by solar heat storage based on Moroccan irradiation

Hicham BOUSHABA^{1,*}, Abdelaziz MIMET¹, Mohammed El GANAOU², Abderrahman MOURADI¹

¹Laboratoire d'Energétique, Faculté des sciences. BP 2121, 93000 Tétouan. Maroc.

²LERMAB, Institut Universitaire de Technologie de Longwy, Université de Lorraine, 54400 Cosnes et Romain, France

Abstract. The aim of this paperwork is to provide a performance comparative study of an adsorption refrigeration system powered by solar heat storage based on Moroccan irradiation. The system operates with ammonia as refrigerant and activated carbon as adsorbent. A parabolic through collector is used to collect the solar energy and store it in a heat storage tank. A dynamic simulation program interpreting the real behavior of the system has been developed. The pressure, temperature and adsorbed mass profiles in the Adsorber have been revealed. The system performance is estimated in terms of the specific cooling power (SCP) and the solar coefficient of performance (SCOP). The solar irradiation and the real ambient temperature variations corresponding to the six climatic zones in Morocco are considered. The effect of those conditions on the performance of the system has been investigated. The results show the capability of our system to realize more than one cycle and produce cold during the day. For an optimal configuration of the system and operating conditions of evaporation temperature, $T_{ev}=0$ °C, condensation temperature, $T_{con}=30$ °C and generation temperature, $T_3=100$ °C, the process could achieve a SCP of 151 W.kg^{-1} and its solar COP could attain 0.148. The system performances improve especially in sunny area.

Nomenclature

c	constant characteristic of the gas.
C_i	specific heat of the phase i ($\text{J kg}^{-1} \text{K}^{-1}$)
$C_{p,l}$	specific thermal capacity of the refrigerant ($\text{J kg}^{-1} \text{K}^{-1}$)
$C_{p,steel}$	the specific thermal capacity of steel ($\text{J kg}^{-1} \text{K}^{-1}$)
E_s	the total daily solar energy ($\text{kW h m}^{-2} \text{d}^{-1}$)
h_g	specific enthalpy of ammonia at gaseous phase (J kg^{-1})
U_L	overall heat loss coefficient ($\text{W m}^{-2} \text{K}^{-1}$)
F_R	heat removal factor of the collector
C_r	concentration ratio of the collector
G	solar radiation received by the collector (W m^{-2})
L	vaporization Latent heat of the refrigerant (J kg^{-1})
n	number of adsorbate molecular layers
m_a	adsorbed mass (kg (kg-ac)^{-1})
P	pressure (bar)
P_s	saturated vapor pressure of the adsorbate liquid (bar)
Q_f	quantity of cold produced in the evaporator (J m^{-2})
q_m	mass flow rate of ammonia (kg s^{-1})
d	inner diameter of the tubes (m)
r	radial coordinate (m)
s	thickness of the tube (m)
T	temperature of adsorbent (K)
T_{amb}	ambient temperature (K)
t	time (s)

u_i specific internal energy of the phase i (J kg^{-1})

Greek symbols

ΔH_{ads}	the latent heat of adsorption (J kg^{-1})
Δm	cycled mass of the refrigerant (kg m^{-2})
ϵ	bed porosity
η_0	optical solar efficiency of the collector
λ_e	equivalent thermal conductivity coefficient ($\text{W m}^{-1} \text{K}^{-1}$)
ρ_i	density of the phase i (kg m^{-3})
ρ_{steel}	the density of steel (kg m^{-3})
α	volume fraction of the adsorbed phase

Subscripts

i	gas, solid or adsorbed gas
ads	adsorption
con	condensation, condenser
ev	evaporation, evaporator

Abbreviations

AC	activated carbon
SCOP	solar coefficient of performance
SCP	specific cooling power
TDMA	Tri-Diagonal Matrix Algorithm

* Corresponding author: boushaba@gmail.com

1. Introduction

Currently, a variety of cooling technologies is available in market. Many of these technologies are not ecological friendly. Most of the refrigerants (CFC, HFC, HCFC...) used in these conventional technologies is not healthy for the environment and without high performance to reduce CO₂ emissions contributing to the greenhouse effect[1][2]. Another concern regarding this technology is the availability of electricity especially in rural areas.

Thus, scientists are interested in alternative technologies that are dedicated to sustainability and the ecological future of our planet. Solar refrigerator systems based on solid adsorption present an interesting solution. Many theoretical and experimental studies [3][4][5] have demonstrated the feasibility of such machines in the Moroccan climate.

The most studied pairs of solar adsorption refrigeration machines are ammonia/ activated carbon [6], methanol/activated carbon [7], fiber-ethanol/activated carbon [8], water/zeolite [9] and Water/Silica Gel [10]. All these machines work with an intermittent adsorption cycle, however, the presented system could surmount this character.

This study proposes a performance comparative analyze of a solar adsorption refrigerator based on heat storage that is collected by a parabolic through collector and where the pair adsorbent/adsorbate is activated carbon/ammonia.

In this paperwork, the model identifies the influence of the six climatic zones in Morocco on the performance of the system.

2. System and process description

Fig.1 illustrate schematically the system, it is constituted of a cylindrical adsorber containing the activated carbon-ammonia, an evaporator inside cold room, a condenser, reservoir of ammonia, refrigerant valves, a solar concentrator (PTC), a heat storage tank, a cold storage tank and circulating pump.

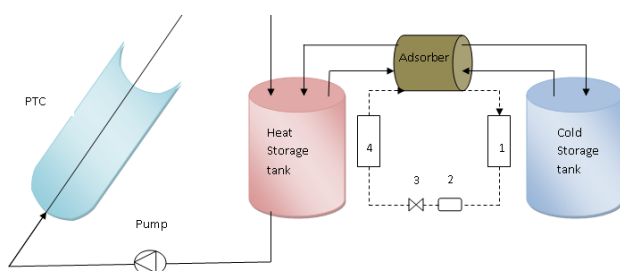


Fig. 1. Schematic diagram of the solar adsorption refrigerator driven by the PTC: 1. Condenser; 2. Ammonia reservoir; 3. Expansion valve; 4. Evaporator-cold room.

For generating cold continuously, the adsorber has to accomplish several successive adsorption cycles. The operation of the adsorber can be reported as follows. When the adsorbent (at temperature T) is in touch with the vapor of the refrigerant (at pressure P), an amount m_a of refrigerant is stuck inside the pores in an adsorbate state.

This adsorbed mass is function of T and P according to a bi-variant equilibrium $m_a=f(T,P)$. Furthermore, for a fixed pressure, the aptness of m_a decreases as T increases, while for a fixed adsorbed mass, the pressure P increases with T . It occurs the opportunity to carry out an ideal refrigerating cycle including of a phase of heating/desorption-condensation followed by a phase of cooling/adsorption-evaporation Fig.2.

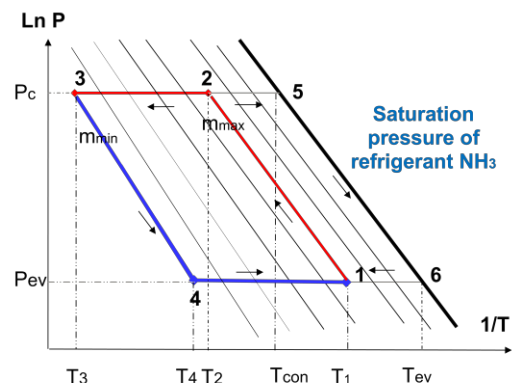


Fig. 2. The Clapeyron diagram: the ideal adsorption cycle of NH₃.

In the start of the cycle, the adsorbent bed is heated up to the temperature T_2 and then desorbs refrigerant into the condenser under high temperature and high pressure, until it reaches the maximal temperature T_3 fixed by the hot HTF. At that time, the adsorber is cooled down by the cold HTF till the temperature T_4 and adsorbs refrigerant vapor from the evaporator under low temperature and low pressure. Consequently the cooling effect is engendered in the cold room. When the adsorbent bed attains its minimum temperature fixed by the cold HTF, a new cycle lead off.

3. Quantitative approach by modelling

The model developed in this study reproduces the transitory behavior of the adsorbent bed. It makes involve of the conservation equations of energy and mass of the refrigerant in the adsorbent bed. The model calculates the solar performances of the system. The model of heat and mass transfer hold in this study has been proved by experimentation in the initial work that was done by A. Mimet [11].

3.1 Model hypothesis:

The main model suppositions appropriated in this study are as follows:

- (1) The pressure within the adsorber is uniform.
- (2) The adsorption/desorption process is an isobaric process.
- (3) The porous medium properties have a cylindrical symmetry.
- (4) The conduction heat transfer in the porous medium can be characterized by an equivalent thermal conductivity, λ_e .
- (5) The heat transfer is radial and the convection heat transfer due to the radial mass transfer is sloppy.
- (6) The temperature of HTF is uniform.

- (7) For the period time, all phases are in mechanical, chemical and thermal local equilibrium.
- (8) The gaseous phase acts as an ideal gas.
- (9) The evaporator and the condenser are ideal: T_{ev} and T_{con} are invariable through the isobaric phases.

3.2 Model equations:

In view of the hypothesis specified ahead of, a transitory model based on harmonized heat and mass transfer and the adsorption process in the porous medium and on the energy balance of the collector and the HST is elaborated. The model equations are clarified in the succeeding sections.

3.2.1 Thermal analysis of the solar sensor: Parabolic trough collector and Heat storage tank modelling:

The thermal efficiency of a PTC is determined as the proportion of the useful energy generated over any period time to the irradiation incident on the sensor aperture over the same period. It can be determinate from the 'Hottel-Whillier-Bliss' equation:

$$\eta = F_R \eta_0 - \frac{F_R U_L (T_{in} - T_{amb})}{C_r I} \quad (1)$$

Moreover, the instantaneous efficiency of the collector can be also indicated in function of the temperature gain obtained in the sensor by the subsequent formula:

$$\eta' = \frac{\dot{m}_f C_{pf} (T_{out} - T_{in})}{I W L_c} \quad (2)$$

T_{out} is the HTF temperature in the sensor outlet. Eq. (1) and Eq. (2) allows the calculation at each instant T_{out} versus T_{in} . The energy balance equation in the HST assesses the temperature of the HST as follow:

$$(M_{hst} C_{pf} + M_{me} C_{pme}) \frac{dT_{hst}}{dt} = \dot{m}_f C_{pf} (T_{out} - T_{in}) + UA_{hst} (T_{amb} - T_{hst}) \quad (3)$$

Whither M_{hst} is the mass of HTF in the HST, C_{pf} is the specific heat of HTF in the HST and T_{hst} is the temperature of HTF in the HST. M_{me} is the HST metal mass and C_{pme} is its specific heat, while (UA_{hst}) is the loss coefficient area product of the HST. The first term to the right side of Eq. (3) means the thermal contribution from the PTC.

3.2.2 Heat and mass transfer equations in the adsorber: Mass conservation equation:

The mass conservation of the refrigerant within the control volume of the adsorber (a layer of radial coordinate r and thickness dr) yields:

$$\frac{\partial}{\partial t} [2\pi r dr [(\varepsilon - \alpha)\rho_g + \alpha\rho_a]] = -q_m(r, t) + q_m(r + dr, t)$$

$$= \left(\frac{\partial q_m}{\partial r}\right) dr \quad (4)$$

Whither q_m is the refrigerant flow rate inside the layer of the control volume.

3.2.3 Energy balance equation:

Energy equation that reveals the energy balance in the layer of the adsorbent bed of a thickness dr and a length of one meter is stated by the following:

$$\begin{aligned} \frac{\partial}{\partial t} [2\pi r dr [(1 - \varepsilon)\rho_s u_s + (\varepsilon - \alpha)\rho_g u_g + \alpha\rho_a u_a] \\ + q_m(r, t) \cdot h_g(T(r), P) \\ - q_m(r + dr, t) \cdot h_g(T(r + dr), P) \\ = 2\pi r dr \lambda_e \left[\frac{\partial^2 T}{\partial r^2} + \frac{1}{r} \frac{\partial T}{\partial r} \right] \end{aligned} \quad (5)$$

λ_e is the equivalent thermal conductivity given by[11], it is equivalent to $0.348 \text{ Wm}^{-1}\text{K}^{-1}$. The refrigerant adsorbed mass is a function of both pressure and temperature of the porous medium, it is estimated with the model of Brunauer–Emmett and Teller (B.E.T)[12]:

$$\frac{m_a}{m_0} = \frac{c \cdot x}{(1-x)} \times \frac{1 - (n+1) \cdot x^n + n \cdot x^{n+1}}{1 + (c-1) \cdot x - c \cdot x^{n+1}} \quad (6)$$

Whither m_a is the adsorbed mass at the relative pressure P/P_s ; m_0 is the adsorbed mass required to form a monomolecular layer; $x = P/P_s$ is the relative pressure; P is the pressure at the equilibrium; P_s is the adsorbate liquid saturated vapor pressure; c is a gas characteristic constant and n is the number of the adsorbate molecular layers.

3.2.4 General equation of heat and mass transfer inside the adsorbent bed:

The heat and mass transfer equation in the adsorbed bed is established by incorporating the mass conservation and the energy balance equations i.e. Eqs. (4) and (5), which is:

$$\begin{aligned} \left[(1 - \varepsilon)\rho_s C_s + (\varepsilon - \alpha)\rho_g C_g + \alpha\rho_a C_a \right] \frac{\partial T}{\partial t} \\ = \lambda_e \left[\frac{\partial^2 T}{\partial r^2} + \frac{1}{r} \frac{\partial T}{\partial r} \right] \\ + \frac{\partial}{\partial t} [(\varepsilon - \alpha)\rho_g] \frac{P}{\rho_g} + \frac{1}{2\pi r dr} \left(\frac{P}{\rho_a} + \Delta H_{ads} \right) \left(\frac{\partial m_a}{\partial t} \right) \end{aligned} \quad (7)$$

ΔH_{ads} is estimated using the Clausius–Clapeyron equation[13]:

$$\Delta H_{ads} = RT^2 \left(\frac{\partial \ln P}{\partial T} \right)_{m_a}$$

Whither R is the adsorbate gas constant.

Eq. (7) has been recorded for all the tube layers yielding a nonlinear system of partial derivative equations; it is concluded with boundary and initial conditions. This nonlinear system can be resolved numerically with a method of implicit finite difference.

3.2.5 Initial and Boundary conditions:

For completing the model mathematical formulation, the boundary and initial conditions are notified as follow:

Initial condition :

$$T(r, 0) = T_1 = 20 \text{ } ^\circ\text{C} \quad (r=0, \dots, R_{\text{tube}})$$

Whither $T(r, 0)$ is the adsorbent bed layer temperature of radius r at the time $t = 0$, R_{tube} is the tube radius and T_1 is the adsorbent bed minimal temperature.

Boundary condition:

- For ($r=0$)

$$\left(\frac{\partial T}{\partial r}\right)_{r=0} = 0$$

This situation states the temperature gradient nullity at the axis of the tube.

- For ($r=R_{\text{tube}}$)

$$\left(\frac{\partial T}{\partial r}\right)_{r=R_{\text{tube}}} = h_{gl}(T_{\text{HTF}} - T)$$

h_{gl} is the coefficient of the global heat transfer among the porous medium and the HTF.

Further, the thermodynamic equilibrium properties of the adsorbent bed are taken from the literature: the adsorbent activated carbon[14], the refrigerant ammonia gas[15] and the adsorbed ammonia[16], although the climatic data employed in this simulation correspond to a usual summer day of July, reported from the six climatic zones of Morocco as shown in Fig.3 and Fig.4.

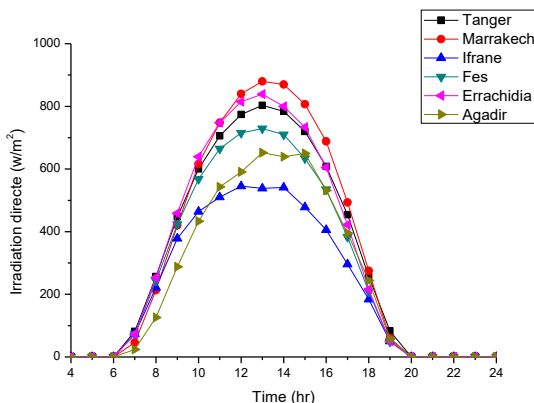


Fig. 3. Daily direct irradiation of the six climatic zones

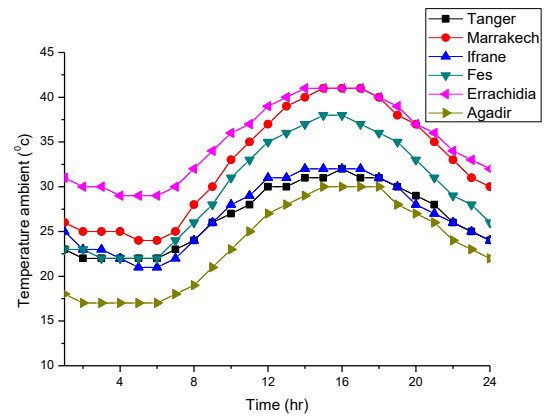


Fig. 4. Ambient temperature variation of the six climatic zones

3.3 Performance investigation:

The performance evaluation parameters of the adsorption-refrigerating machine used in this study are the specific cooling power (SCP) and the solar coefficient of performance (SCOP). These parameters are specified by the following expressions:

3.3.1 The solar performance coefficient:

Usually, the efficiency of a solar refrigerating machine is estimated by the solar coefficient of performance (SCOP), it is an assessment to find how the solar thermal energy is efficiently transformed to a useful cooling effect. It is given as:

$$SCOP = \frac{Q_f}{E_s}$$

Where Q_f is the generation of cooling in the evaporator through an adsorption cycle. This quantity is equivalent to the evaporation latent heat of the refrigerant minus the sensible heat to cool down the refrigerant from T_{con} the temperature of condensation to T_{ev} the temperature of evaporation:

$$Q_f = m_{ac}\Delta m \left[L(T_{ev}) - \int_{T_{ev}}^{T_{con}} C_{p,l} dT \right]$$

With $L(T_{ev})$ is the vaporization latent heat of the refrigerant at temperature T_{ev} and $C_{p,l}$ is the specific thermal capacity of the refrigerant, m_{ac} is the mass of adsorbent in the adsorber, Δm is the cycled adsorbate mass. Δm can be calculated by using (B.E.T.) (6) formula as follows:

$$\Delta m = m_{\text{max}} - m_{\text{min}}$$

E_s is the total daily solar energy:

$$E_s = \int_{t_{sr}}^{t_{ss}} G(t)A_s dt$$

Where $G(t)$ is the solar irradiance. A_s is the sensor area, t_{sr} is the time of sunrise and t_{ss} is time of sunset. The Fig.5 illustrates the variation of the total daily solar energy for the six climatic zones of Morocco represented by six cities.

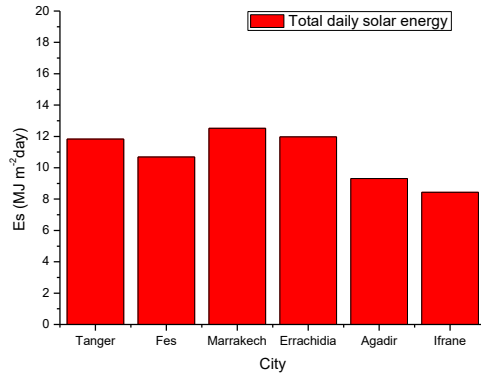


Fig. 5. Variation of the total daily solar energy

3.3.2 The Specific cooling power:

The SCP is determined as the proportion of the cooling generation and the adsorbent mass per the cycle time:

$$SCP = \frac{Q_f}{m_{act} t_{cycle}}$$

4. Numerical resolution

For resolving the system of the differential equations associated to the porous medium, a numerical method premised on both an entirely implicit scheme and the finite differences technique is employed. The discretized equations are resolved with a TDMA method (the Tri-Diagonal Matrix Algorithm); in addition, iterative techniques are used to resolve the nonlinearity of the equations. A numerical tool elaborated in FORTRAN has been established in order to simulate the behavior of the solar adsorption-refrigerating machine.

5. Results and discussion

A numerical examination is carried out under the design and operating conditions enumerated above. The simulation results are exposed graphically.

5.1 Solar heat storage:

For a configuration of the mass flow rate in the sensor piping equal to $0.01 \text{ kg}\cdot\text{s}^{-1}$ and 0.015 m^3 as volume of the heat storage tank (HST). Fig.6 corresponds to the daily variation of the HST mean temperature (T_{hst}) according to the real climatic data employed in the simulation. It is observed that, the HST temperature (T_{hst}) could fulfill the operating of the system by the sensor for a prolonged period of time; it is equal to 2.5 hours in Ifrane and could attain 9.3 hours in Marrakech, through this time, the heat storage tank (HST) could supply the adsorber with the necessary temperature of heating about 100 C° .

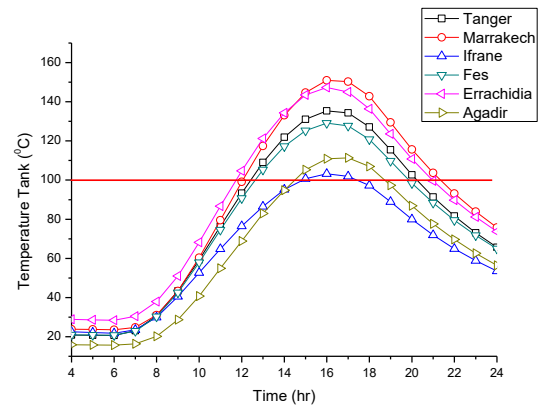


Fig. 6. Variation of the temperature of the heat storage tank

5.2 Pressure and adsorbed mass inside the adsorbent bed:

Fig. 7 describes the progression of the adsorbed mass and the pressure through the period time of one cycle. It illustrates that the pressure of the adsorbent bed augments from the initial value equal to 4.2 to the value of 11.6 bars, whereas the adsorbed mass held a constant value equal to $0.136 \text{ kg kg-AC}^{-1}$. The pressure stays constant at the high pressure of 11.6 bars to the end of the phase of heating, resulting to an important diminishing in the adsorbed mass until the value of $0.082 \text{ kg kg-AC}^{-1}$. Throughout the phase of cooling, the pressure reduces to attain the initial value equal to 4.2 bars. At this instant the adsorbed mass kept a constant value equal to $0.082 \text{ kg kg-AC}^{-1}$. Then the pressure remains constant at the low pressure of 4.2 bars whereas the adsorbed mass augments to attain the value of $0.119 \text{ kg kg-AC}^{-1}$.

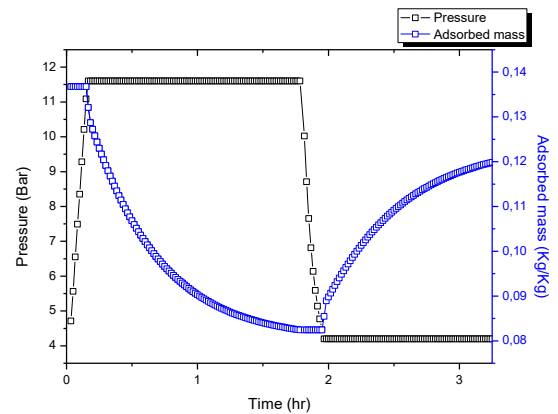


Fig. 7. Evolution of pressure and adsorbed mass with time (adsorber diameter=0.02m)

5.3 Performance evaluation:

According to the obtained results of the solar heat storage, Fig.8 presents the variation of the SCOP and the SCP of the system. It can be seen that, the SCOP reduce from 0.148 to 0.057, it correspond to cities of Errachidia and Ifrane respectively. On the other hand, the SCP of the refrigeration system can reach a value of $151 \text{ W}\cdot\text{kg}^{-1}$ in the city of Marrakech. This trend results because, as longer is the period of time to supply the adsorber, the number of

cycles accomplished during the availability of the solar energy is bigger.

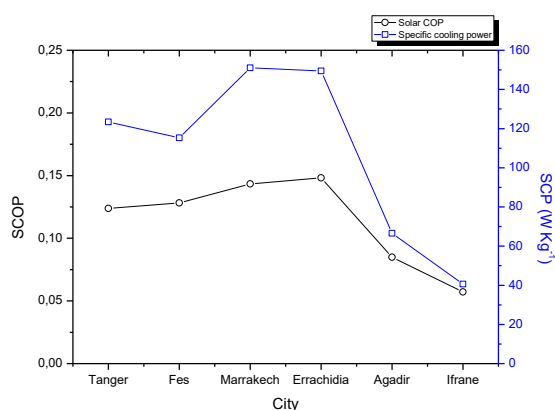


Fig. 8. Performance comparison between the six climatic zones of Morocco

6. Conclusion

In this study, a model simulating the real behavior of a solar adsorption refrigerator powered by a parabolic trough collector (PTC) has been established, in order to accomplish successive adsorption cycles. This model premised on the heat balance equations in the collector components and on the heat and mass transfer in the adsorbent bed has been used. The proposed numerical program computes the Specific cooling power (SCP) and the solar coefficient of performance (SCOP) in order to evaluate the system performance for the six climatic zones. The results show a great sensitivity of the SCP and the SCOP of the machine to the solar irradiation and the real ambient temperature variations. Within the ranges of analysis, the results of simulation demonstrate that optimal performance values are acquired especially in sunny area. This work proves that the PTC is a valuable component, for enhancement of solar adsorption refrigeration systems. The acquired results confirmed the possibility to generate cold during the day and consequently to surmount the intermittent character of the solar adsorption refrigeration machines.

Key words

Adsorption, Cooling system, Solar Energy, Heat transfer, heat storage.

Acknowledgment

Many thanks to the PHC Maghreb program for the financial support and Distinguished Professors coordinators of this project for their precious technical efforts.

References

[1] J. M. Calm, "Emissions and environmental impacts from air-conditioning and refrigeration systems," *Int. J. Refrig.*, vol. 25, pp. 293–305, 2002.
 [2] V. Vakiloroyaya, B. Samali, and K. Pishghadam,

"A comparative study on the effect of different strategies for energy saving of air-cooled vapor compression air conditioning systems," *Energy Build.*, vol. 74, pp. 163–172, 2014.
 [3] A. Boubakri, M. Pons, F. Meunier, and J. J. Guilleminot, "Experimental study of adsorptive solar – powered ice makers in Agadir (Morocco) – 1. Performance in actual site.," *Renew. Energy*, vol. 2, no. 1, 1992.
 [4] A. Al Mers, A. Azzabakh, A. Mimet, and H. El Kalkha, "Optimal design study of cylindrical finned reactor for solar adsorption cooling machine working with activated carbon – ammonia pair," *Appl. Therm. Eng.*, vol. 26, pp. 1866–1875, 2006.
 [5] A. El Fadar, A. Mimet, and M. Perez-Garcia, "Modelling and performance study of a continuous adsorption refrigeration system driven by parabolic trough solar collector," *Sol. Energy*, vol. 83, pp. 850–861, 2009.
 [6] M. Louajari, A. Mimet, and A. Ouammi, "Study of the effect of finned tube adsorber on the performance of solar driven adsorption cooling machine using activated carbon – ammonia pair," *Appl. Energy*, vol. 88, no. 3, pp. 690–698, 2011.
 [7] F. Meunier, "Theoretical performances of solid adsorbent cascading cycles using the zeolite-water and active carbon-methanol pairs: four case studies," *heat Recover. Syst.*, vol. 6, no. 6, pp. 491–498, 1986.
 [8] B. B. Saha, I. I. El-Sharkawy, A. Chakraborty, and S. Koyama, "Study on an activated carbon fiber-ethanol adsorption chiller : Part I - system description and modelling," *Int. J. Refrig.*, vol. 30, pp. 86–95, 2007.
 [9] M. Pons and J. J. Guilleminot, "Design of an Experimental Solar- Powered , Solid-Adsorption Ice Maker," *J. Sol. Energy Eng.*, vol. 108, pp. 332–337, 1986.
 [10] D. C. Wang and J. P. Zhang, "Design and performance prediction of an adsorption heat pump with multi-cooling tubes," *Energy Convers. Manag.*, vol. 50, no. 5, pp. 1157–1162, 2009.
 [11] A. Mimet, "«Etude Théorique et expérimentale d'une machine Frigorifique à adsorption d'Ammoniac sur Charbon Actif»,» Faculty Polytechnic of Mons, 1991.
 [12] S. Brunauer, P. H. Emmett, and E. Teller, "Adsorption of Gases in Multimolecular Layers," *J. Am. Chem. Soc.*, vol. 60, pp. 309–319, 1938.
 [13] Y. Teng, R. Z. Wang, and J. Y. Wu, "Study of the fundamentals of adsorption systems," *Appl. Therm. Eng.*, vol. 17, no. 4, pp. 327–338, 1997.
 [14] CHEMVIRON, "Granular activated carbon," 1988.
 [15] Institut International de Froid, *Tables et diagrammes pour l'industrie du froid, Propriétés thermodynamiques du R12, R22, R717.*, Paris, 1981.
 [16] A. Mahamane, "«Etude de l'adsorption de vapeurs purs sur solides poreux,»" Faculty polythecnic of Mons, 1989.